Organic 2D Materials

Smart Organic Two-Dimensional Materials Based on a Rational Combination of Non-covalent Interactions

*Wei Bai, Ziwen Jiang, Alexander E. Ribbe, and S. Thayumanavan**

Dedicated to Professor Peter Beak on the occasion of his 80th birthday

Abstract: *Rational design of organic 2D (O2D) materials has made some progress, but it is still in its infancy. A class of self-assembling small molecules is presented that form nano/ microscale supramolecular 2D materials in aqueous media. A judicial combination of four different intermolecular interactions forms the basis for the robust formation of these ultrathin assemblies. These assemblies can be programmed to disassemble in response to a specific protein and release its non-covalently bound guest molecules.*

Two-dimensional (2D) materials have attracted great attention owing to their potential in many applications ranging from semiconductors to biomedicine.[1] In contrast to the more prosperous inorganic 2D materials, study of organic 2D (O2D) materials is still in its launching phase, but is believed to be promising owing to their soft characteristics and thus suitability in a variety of biomedical applications.[2] Among the O2D materials, significant efforts have been directed toward graphene analogues.[1a] Although few successful attempts in making polymeric[3] and supramolecular[4] O2D materials have been reported, examples for the effective formation of free-standing ultrathin O2D materials are still quite limited. Also, current mainstream, top-down preparation strategies contain additional exfoliation steps, while the traditional bottom-up methods such as self-assembled monolayer formation rely on pre-organization of molecules at a liquid-air interface or on a substrate surface.[5] Thus, the development of a facile molecular design strategy for the preparation of ultra-thin O2D materials addresses an urgent need with both fundamental and practical implications.

Moreover, though research on making organic–inorganic hybrid smart 2D materials[6] has become a hotspot in recent years, studies on pure organic smart 2D materials are still quite rare.[7] Thus, designing organic smart 2D crystalline materials with stimuli-sensitive characteristics, especially

biomolecule sensitivity, remains a challenge. Herein, we report a simple bottom-up strategy, which uses multiple supramolecular interactions in a concerted fashion, to prepare smart O2D materials by non-interfacial self-assembly of organic small molecules in aqueous media at room temperature (Scheme 1).
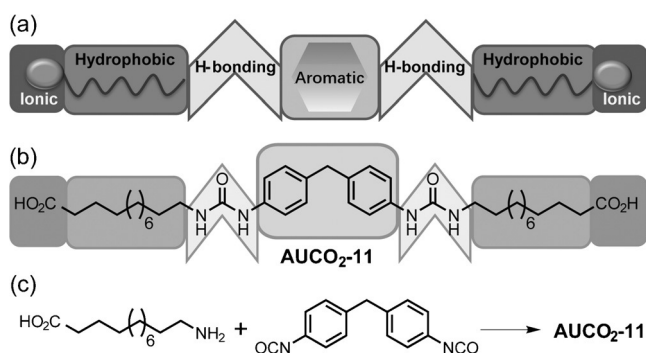

Scheme 1. a) Illustration of the molecular design containing four complementary intermolecular interactions. b) Example of a molecule for the formation of the 2D assemblies in the aqueous phase. c) Example of the simplicity in the synthesis to achieve the targeted materials.

We show that these autonomously-formed mono/few-layer thick O2D sheets require no extra exfoliation. We also show that these O2D sheets can be programmed to disassemble in response to a specific protein. Since small hydrophobic guest molecules can be loaded into these sheets, this binding-induced disassembly process can be conveniently visualized.

To fundamentally unravel the factors that influence the formation of the O2D structures, a concerted series of twelve molecules has been designed (Scheme 2) and synthesized using a simple approach (Scheme 1 c). The basic molecular design strategy here involves three parts: a) the utility of hydrogen bonding interactions that are proximally located with aromatic rings to have correlated hydrogen-bonding and π–π interactions; in fact, molecules with similar structure have been reported as small molecule gelators, owing to the self-assembly ability provided by strong interactions;[8a] b) an alkyl chain linking the urea-based aromatic units with an ionic head group, where the alkyl chain provides the hydrophobic interactions to reinforce the assembly in the aqueous phase; and c) the ionic head groups on either side of the molecules to introduce repulsive forces that presumably mitigate inter-

[*] Dr. W. Bai, Z. Jiang, Prof. S. Thayumanavan
Department of Chemistry, University of Massachusetts Amherst
Amherst, MA 01003 (USA)
E-mail: thai@chem.umass.edu
Dr. A. E. Ribbe
Department of Polymer Science and Engineering
University of Massachusetts Amherst
Amherst, MA 01003 (USA)
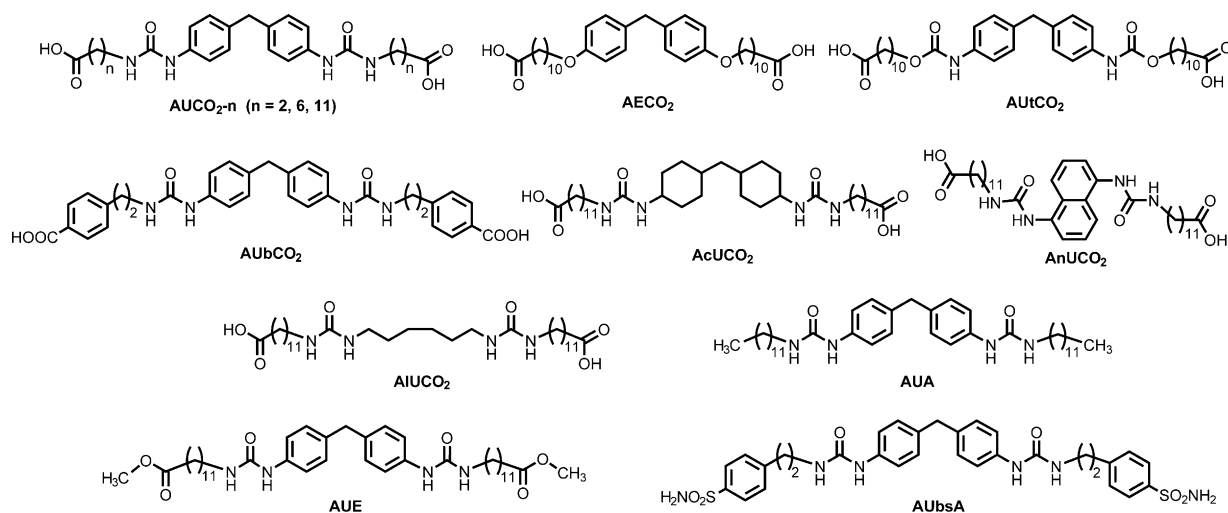
Scheme 2. Structure of the aromatic urea (AU) based amphiphiles and the appropriate controls to test the design principles.

layer interactions and thus avoid the need for exfoliation steps to achieve ultrathin O2D sheets.

The O2D sheets were prepared by simply injecting a DMSO-based solution of the small molecules into deionized water. The resultant suspensions were allowed to stand still for about 12 hours to let the automated self-assembly finish. These samples were then analyzed by transmission electron microscopy (TEM), high-resolution TEM (HRTEM), scanning electron microscopy (SEM), and atomic force microscopy (AFM). $AUCO_2$-11 was investigated first, since the relatively long alkyl chains on both sides may provide for the

Figure 1. Microscopy analyses of AUCO2-11. a) TEM image of the 2D sheets in water; b) HRTEM image of the 2D sheets in water with a zoomed in image on upper-right corner; c) SEM images of 2D sheets (Au-coated); d) AFM image with height profiles; and e) histogram of height distribution. Scale bars: a) 1 μm, b) 8 nm, (zoomed-in image: 4 nm), c) 1 μm, d) 10 μm, e) 5 μm.
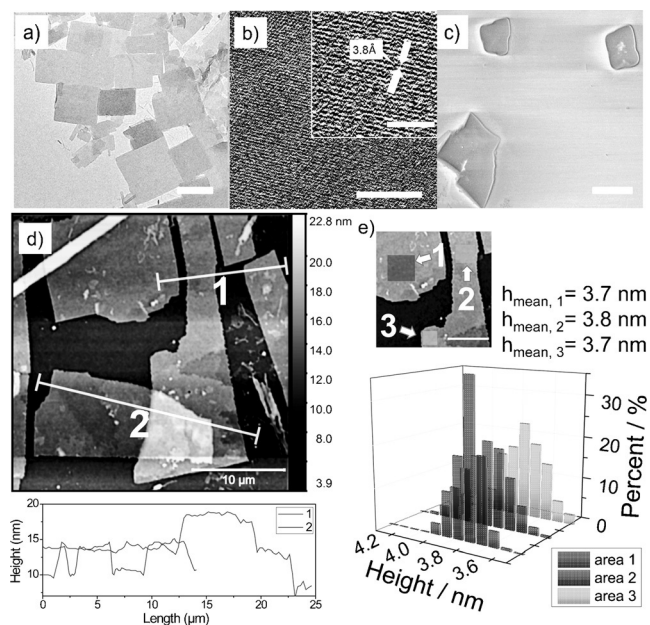
targeted self-assembly due to strong hydrophobic effect and van der Waals interactions.

TEM and HRTEM images show that $AUCO_2$-11 form 2D sheets and that the structures are highly ordered (Figure 1 a and b). The distance of the visible lattice fringes roughly corresponds to about 0.376 nm, in agreement with the interspacing of $(10\bar{1}0)$ planes (0.38 nm). The corresponding selected area electron diffraction (SAED) pattern (Supporting Information, Figure S1d) displays clear phases, suggesting the high crystal quality within the 2D sheet. SEM images further support the formation of the O2D structure (Figure 1 c).

The fact that these O2D sheets were stably formed with or without the gold-coating in SEM suggests that the O2D assembly is robust (Supporting Information, Figure S1a). AFM studies also suggest that the O2D sheets are relatively smooth with lateral dimension at micrometer scale (Figure 1 d). Average thickness of these sheets, based on AFM height profiles, reveals their relatively uniform thickness of (3.7 ± 0.1) nm. A statistical study of the monolayer thickness suggests a mean average height of about 3.7 nm (Figure 1 e). XRD investigation also suggests a highly ordered structure with a *d*-spacing of 3.7 nm (Supporting Information, Figure S1b) which matches the results of small angle X-ray scattering (SAXS) of the 2D sheets in powder form (Supporting Information, Figure S1e). Note that shape and size control is not a current target for this O2D self-assembly and will be the focus of future work.

As an initial test to identify whether this is a hydrophobicity-induced self-assembly, formation of 2D assemblies in pure DMSO was tested and was found that these do not provide any significant assembly (Supporting Information, Figure S1c). To further understand the design rules in aqueous media, compared to those in organic solvents,[8] we systematically varied the structure of the molecule.

First, the effect of the hydrophobic linker was studied by comparing $AUCO_2$-2 and $AUCO_2$-6 with $AUCO_2$-11. The self-assembly was performed at three different pH values and the longer linkers favored the 2D structure in all cases

Table 1: Comparison of AUCO$_2$-1 and AUbCO$_2$ in their assembly behavior in aqueous solution.

Name	pH 4	pH 7	pH 12
AUCO$_2$-2	nanosheets or defective sheets	no film or defective film	no film
AUCO$_2$-6	µm sheets	µm sheets or defective film	no film or defective film
AUCO$_2$-11	µm sheets	µm sheets	µm ribbon or defective film
AUbCO$_2$	µm sheets	µm sheets	µm ribbon or defective film

(Table 1). This is attributed to the increasing hydrophobic effect and van der Waals interactions, akin to those seen in surfactant self-assembly. Interestingly AUbCO$_2$, containing a benzoic acid as head group in addition to only a two carbon linker, also exhibits a strong propensity to form 2D assemblies. This may be due to the additional reinforcement provided by π–π interactions. The self-assembly variations observed at different pH values is likely due to the optimal balance between the head-group repulsions that could prevent the 2D self-assembly and that are necessary to prevent interlayer interactions to provide the targeted ultra-thin structures. In fact, these molecules were found to form highly aggregated 2D structures at pH < 4.

The coordinated use of multiple interactions to drive the formation of the O2D assemblies is the basis for our molecular design. To test this, we examined the importance of the intermolecular hydrogen bonding due to the urea functionalities. Specifically, we replaced the urea moieties with ether (AECO$_2$) or urethane (AUtCO$_2$) functionalities, where the hydrogen-bonding interaction is completely obviated or partially weakened, respectively. Indeed, the assemblies were irregular aggregates in both cases (Figure 2a,b).
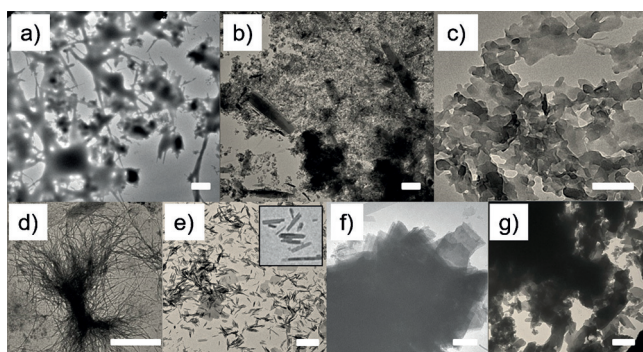
Figure 2. SEM images of assemblies of a) AECO$_2$, b) AUtCO$_2$, c) AcUCO$_2$, d) AlUCO$_2$, e) AnUCO$_2$ with a zoomed-in image on upper-right corner, f) AU, and g) AUE in water. Scale bars: 1 µm.

These results suggest that the urea units, with their hallmark hydrogen-bonding self-complementarity, are critical for the observed 2D assemblies.

Next, we investigated the importance of the rigid aromatic units at the core. AcUCO$_2$, where the two phenyl rings were replaced by cyclohexyl units, afforded assemblies with significant crosslinking (Figure 2c). Though the remnant rigidity in the structure allowed 2D growth, the loss of the assortative π–π interactions seems to have increased the interlayer interactions, which is presumably due to mismatched hydrogen-bonding interactions, to cause crosslinking among the layered structures. On the other hand, if a completely flexible alkyl spacer is used (as in AlUCO$_2$), needle-like structures were observed, indicative of a linear propagation of the assemblies (Figure 2d). These assemblies were also bundled or aggregated, which is presumably due to mismatched interactions among the linear assemblies. Interestingly, there seems to be a need for a small amount of flexibility between the two urea units. If there is no flexibility in the spacer, as with AnUCO$_2$, small ribbon-like assemblies were formed (Figure 2e). This is attributed to the possibility that the naphthyl units are too rigid as a linker, where the hydrogen-bonding interaction and the aromatic π–π interaction directions are not complementarily placed.

We hypothesized that optimal head-group repulsion is needed to balance the 2D assembly formation and the prevention of interlayer interactions. To test this hypothesis, we replaced the carboxylate moiety with an alkyl group or masked it as an ester in the form AUA and AUE, respectively. Consistent with our design hypothesis, both molecules exhibited a strong tendency to form 2D structures, but a very limited amount of free-standing mono/few-layer can be observed. Majority of the 2D sheets were stacked together and formed bulk aggregates (Figures 2f,g). These results suggest that the hydrophilic head groups are necessary to avoid the extra exfoliation steps to achieve ultra-thin 2D assemblies.

As a preliminary demonstration of the utility of these O2D materials, we tested these molecules for binding-induced disassembly in response to specific proteins. Binding-induced disassembly has been previously demonstrated with micelle-like amphiphilic aggregates.[9] We conceived that such a demonstration with O2D assemblies will greatly expand the repertoires of both the 2D scaffold and the protein-triggered disassembly process. We employed a benzenesulfonamide moiety, a well-known ligand for carbonic anhydrases,[10] as the surface-exposed functionality in the self-
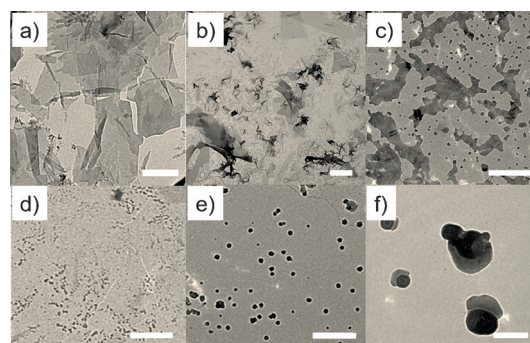

Figure 3. TEM image of AUbsA 2D sheet a) in water, and after incubation of the assembly with the target protein, BCA, for b) 2 hours, c) 4 hours, d) 2 days. TEM images of e) 7 days after addition of control protein, f) a zoom-in image of (e). Scale bars: a)–e) 1 µm, f) 0.1 µm.

assembling small molecule (AUbsA). We first ascertained that this molecule indeed forms a 2D assembly based on TEM, SEM, AFM, and XRD (Figure 3a; Supporting Information, Figure S2a). The O2D sheets were found to be about 2.4 nm thick, which is close to the single-molecule dimension.

When bovine carbonic anhydrase (BCA) was added to an aqueous suspension containing the 2D sheets ($C_{AUbsA} = 1.5 \mu M$), the morphology of the 2D assembly seems to be compromised over time (Figure 3b–d). TEM studies confirmed that majority of these 2D assemblies were completely dissolved at longer time scales. However, the morphological change was also observed for proteins that are non-complementary to the sulfonamides, namely avidin and hyaluronidase. Interestingly, this non-specific interaction produced a consistently spherical nanoparticle morphology that persisted even after two weeks (Figure 3e,f).

Considering the difference in the persistence of the protein-induced morphologies, we tested the possibility of releasing hydrophobic guest molecules within these assemblies in the presence of specific proteins. Accordingly, we loaded pyrene within 2D sheets, where the overall 2D structure was maintained after guest loading (Figure 4a).
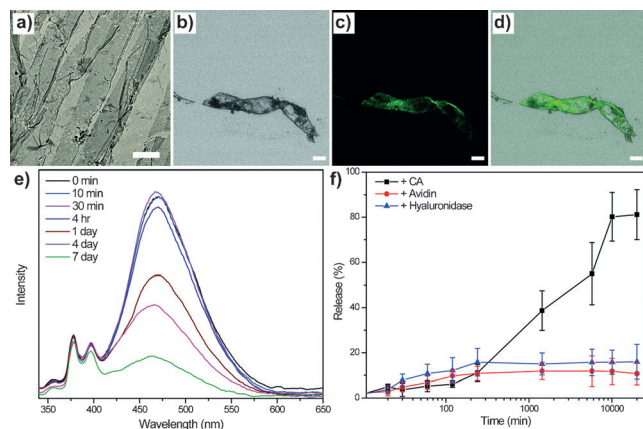
Figure 4. TEM images of AUbsA a) after loading of the pyrene. Confocal images of the 2D sheet, b) bright field, c) pyrene, d) merged image of (b) and (c). e) Pyrene release from 2D sheet in the presence of BCA. f) Plot of percentage release with time and comparison with controls. Scale bars: a) 5 μm, b)–d) 10 μm.

Confocal microscopy also shows that the fluorescent dyes were successfully loaded to the sheets (Figure 4b–d). When the suspension of 2D sheet was exposed to BCA, the possible release of pyrene was monitored by absorption spectroscopy. Since the hydrophobic guest is insoluble in water, it would simply precipitate out of solution. Indeed, the absorbance of pyrene decreased over time in the presence of BCA (ca. 80% release over a few days, Figure 4e and f). No such release was observed in the absence of BCA or in the presence of non-complementary proteins. These observations suggest that a sustained specific protein-responsive release of guest molecules is indeed possible.

In conclusion, we have designed and synthesized a new series of self-assembling molecules that readily afford molecular-thin O2D materials in aqueous media. We show here that

aromatic π–π interactions, hydrogen-bonding interactions, hydrophobic interactions, and electrostatic repulsions all play a key role in the formation of these assemblies. Finally, to the best of our knowledge, there has been no report on smart O2D materials before. By employing a protein-specific ligand as the hydrophilic head group, we have shown that these 2D sheets can undergo a binding-induced disassembly in response to a specific protein. This feature, the simplicity of the synthesis/ preparation method, and our understanding of the factors that underlie the assembly formation provide a foundation for pursuing O2D assemblies for future applications in smart materials-based systems.

[1] a) X. Zhuang, Y. Mai, D. Wu, F. Zhang, X. Feng, *Adv. Mater.* **2015**, *27*, 403–427; b) D. Chimene, D. L. Alge, A. Gaharwar, *Adv. Mater.* **2015**, *27*, 7261–7284; c) S. Butler, S. Hollen, L. Cao, et al., *ACS Nano* **2013**, *7*, 2898–2926; d) P. Miró, M. Audiffreda, T. Heine, *Chem. Soc. Rev.* **2014**, *43*, 6537–6554; e) A. Guptaa, T. Sakthivela, S. Seal, *Prog. Mater. Sci.* **2015**, *73*, 44–126.

[2] a) C. E. Boott, A. Nazemi, I. Manners, *Angew. Chem. Int. Ed.* **2015**, *54*, 13876–13894; *Angew. Chem.* **2015**, *127*, 14082–14101; b) Z. Xiang, D. Cao, *Polym. Chem.* **2015**, *6*, 1896–1911; c) Z. Wang, W. Zhu, Y. Qiu, X. Yi, A. Bussche, A. Kane, H. Gao, K. Koski, R. Hurt, *Chem. Soc. Rev.* **2016**, Advance Article.

[3] a) A. Keller, *Philos. Mag.* **1957**, *2*, 1171–1175; b) K. Nam, S. Shelby, P. Choi, A. Marciel, R. Chen, L. Tan, T. Chu, R. Mesch, B. Lee, M. Connolly, C. Kisielowski, R. Zuckermann, *Nat. Mater.* **2010**, *9*, 454–460; c) H. Zhou, J. Liu, S. Du, L. Zhang, G. Li, Y. Zhang, B. Tang, H. Gao, *J. Am. Chem. Soc.* **2014**, *136*, 5567–5570; d) M. Kory, M. Wörle, T. Weber, P. Payamyar, S. Poll, J. Dshemuchadse, N. Trapp, A. D. Schlüter, *Nat. Chem.* **2014**, *6*, 779–784; e) M. Pfeffermann, R. Dong, R. Graf, W. Zajaczkowski, T. Gorelik, W. Pisula, A. Narita, K. Müllen, X. Feng, *J. Am. Chem. Soc.* **2015**, *137*, 14525–14532; f) X. Zhang, C. Hsu, X. Ren, Y. Gu, B. Song, H. Sun, S. Yang, E. Chen, Y. Tu, X. Li, X. Yang, Y. Li, X. Zhu, *Angew. Chem. Int. Ed.* **2015**, *54*, 114–117; *Angew. Chem.* **2015**, *127*, 116–119.

[4] a) D. Wu, R. Liu, W. Pisula, X. Feng, K. Müllen, *Angew. Chem. Int. Ed.* **2011**, *50*, 2791–2794; *Angew. Chem.* **2011**, *123*, 2843–2846; b) T. Bauer, Z. Zheng, A. Renn, R. Enning, A. Stemmer, J. Sakamoto, A. D. Schlüter, *Angew. Chem. Int. Ed.* **2011**, *50*, 7879–7884; *Angew. Chem.* **2011**, *123*, 8025–8030; c) K. Zhang, J. Tian, D. Hanifi, Y. Zhang, A. C. Sue, T. Zhou, L. Zhang, X. Zhao, Y. Liu, Z. Li, *J. Am. Chem. Soc.* **2013**, *135*, 17913–17918; d) P. Payamyar, K. Kaja, C. Ruiz-Vargas, et al., *Adv. Mater.* **2014**, *26*, 2052–2058; e) G. Wu, P. Verwilst, K. Liu, M. Smet, C. Faulc, X. Zhang, *Chem. Sci.* **2013**, *4*, 4486–4493; f) B. Song, Z. Wang, S.

Chen, X. Zhang, Y. Fu, M. Smet, W. Dehaen, *Angew. Chem. Int. Ed.* **2005**, *44*, 4731 – 4735; *Angew. Chem.* **2005**, *117*, 4809 – 4813.

[5] a) J. Kim, S. Kwon, D. Cho, et al., *Nat. Commun.* **2015**, *6*, 8294; b) N. Wang, Q. Xu, S. Xu, Y. Qi, M. Chen, H. Li, B. Han, *Sci. Rep.* **2015**, *5*, 16764; c) J. Shen, Y. He, J. Wu, C. Gao, K. Keyshar, X. Zhang, Y. Yang, M. Ye, R. Vajtai, J. Lou, P. Ajayan, *Nano Lett.* **2015**, *15*, 5449 – 5454; d) S. Mitra, S. Kandambeth, B. Biswal, et al., *J. Am. Chem. Soc.* **2016**, *138*, 2823 – 2828.

[6] a) B. Yu, X. Jiang, J. Yin, *Chem. Commun.* **2013**, *49*, 603 – 605; b) J. Kim, M. Bohra, V. Singh, C. Cassidy, M. Sowwan, *ACS Appl. Mater. Interfaces* **2014**, *6*, 13339 – 13343; c) R. Mo, T. Jiang, W. Sun, Z. Gu, *Biomaterials* **2015**, *50*, 67 – 74; d) Z. Cao, G. Wang, Y. Chen, F. Liang, Z. Yang, *Macromolecules* **2015**, *48*, 7256 – 7261; e) Y. Hao, L. Wang, B. Zhang, *Nanotechnology* **2016**, *27*, 025101.

[7] a) S. Shin, S. Lim, Y. Kim, *J. Am. Chem. Soc.* **2013**, *135*, 2156 – 2159; b) Y. Zheng, H. Zhou, D. Liu, *Angew. Chem. Int. Ed.* **2013**, *52*, 4845 – 4848; *Angew. Chem.* **2013**, *125*, 4945 – 4948; c) E. Betthausen, M. Dulle, C. Hanske, *Macromolecules* **2014**, *47*, 6289 – 6301; d) C. Lay, M. Lee, H. Lee, I. Phang, X. Ling, *ACS Nano* **2015**, *9*, 9708 – 9717; e) M. Vybornyi, A. Rudnev, R. Häner, *Chem. Mater.* **2015**, *27*, 1426 – 1431.

[8] a) C. Zhang, J. Wang, J. Wang, M. Li, X. Yang, H. Xu, *Chem. Eur. J.* **2012**, *18*, 14954 – 14956; b) R. Davis, R. Berger, R. Zentel, *Adv. Mater.* **2007**, *19*, 3878 – 3881; c) J. Kim, R. Davis, R. Zentel, *J. Colloid Interface Sci.* **2011**, *359*, 428 – 435.

[9] a) J. Guo, J. Zhuang, F. Wang, K. Raghupathi, S. Thayumanavan, *J. Am. Chem. Soc.* **2014**, *136*, 2220 – 2223; b) D. Amado Torres, M. Garzoni, A. Subrahmanyam, G. Pavan, S. Thayumanavan, *J. Am. Chem. Soc.* **2014**, *136*, 5385 – 5399; c) M. Molla, P. Prasad, S. Thayumanavan, *J. Am. Chem. Soc.* **2015**, *137*, 7286 – 7289; d) H. Wang, J. Zhuang, K. Raghupathi, S. Thayumanavan, *Chem. Commun.* **2015**, *51*, 17265 – 17268; e) K. Raghupathi, J. Guo, O. Munkhbat, P. Rangadurai, S. Thayumanavan, *Acc. Chem. Res.* **2014**, *47*, 2200 – 2211.

[10] a) V. M. Krishnamurthy, G. K. Kaufman, A. R. Urbach, I. Gitlin, K. L. Gudiksen, D. B. Weibel, G. M. Whitesides, *Chem. Rev.* **2008**, *108*, 946; b) V. Alterio, A. Di Fiore, K. D'Ambrosio, C. T. Supuran, G. De Simone, *Chem. Rev.* **2012**, *112*, 4421.